Site-Directed Mutagenesis Reveals Transition-State Stabilization as a General Catalytic Mechanism for Aminoacyl-tRNA Synthetases†

Thor J. Borgford,‡ Tamara E. Gray, Nigel J. Brand,§ and Alan R. Fersht*
Department of Chemistry, Imperial College of Science and Technology, London SW7 2AY, U.K.
Received March 26, 1987; Revised Manuscript Received June 23, 1987

ABSTRACT: Some aminoacyl-tRNA synthetases of almost negligible homology do have a small region of similarity around the four-residue sequence His-Ile(or Leu or Met)-Gly-His(or Asn), the HIGH sequence. The first histidine in this sequence in the tyrosyl-tRNA synthetase, His-45, has been shown to form part of a binding site for the γ-phosphate of ATP in the transition state for the reaction as does Thr-40. Residue His-56 in the valyl-tRNA synthetase begins a HIGH sequence, and there is a threonine at position 52, one position closer to the histidine than in the tyrosyl-tRNA synthetase. The mutants Thr → Ala-52 and His → Asn-56 have been made and their complete free energy profiles for the formation of valyl adenylate determined. Difference energy diagrams have been constructed by comparison with the reaction of wild-type enzyme. The difference energy profiles are very similar to those for the mutants Thr → Ala-40 and His → Asn-45 of the tyrosyl-tRNA synthetase. Thr-52 and His-56 of the valyl-tRNA synthetase contribute little binding energy to valine, ATP, and Val-AMP. Instead, the wild-type enzyme binds the transition state and pyrophosphate some 6 kcal/mol more tightly than do the mutants. Preferential transition-state stabilization is thus an important component of catalysis by the valyl-tRNA synthetase. Further, by analogy to the tyrosyl-tRNA synthetase, the valyl-tRNA synthetase has a binding site for the γ-phosphate of ATP in the transition state, and this is likely to be a general feature of aminoacyl-tRNA synthetases that have a HIGH region.

The aminoacyl-tRNA synthetases are a "family" of enzymes responsible for the ligation of amino acids to their cognate tRNAs (Schimmel & Soll, 1979). However, there is no single physical characteristic of the aminoacyl-tRNA synthetases to justify their description as a family in the conventional sense, as, for example, the serine proteases. Their common feature is just that they catalyze the same reaction but for different amino acids and tRNAs. With few exceptions, they are widely varied in molecular mass, subunit composition, and primary sequences. A region of slight homology has been reported near the N-terminus of some of the synthetases for which primary sequences are available, the so-called "HIGH" region [=His-Ile-Gly-His, listed in Borgford et al. (1987)].

The crystal structure of the tyrosyl-tRNA synthetase from *Bacillus stearothermophilus* has been solved (Brick & Blow, 1987). On the basis of this, a combination of site-directed mutagenesis and kinetics has unravelled the mechanism of the first step of the reaction, the formation of the tyrosyl adenylate complex from tyrosine and ATP. The contributions of each of the side chains in the active site to catalysis have been systematically measured, as have those of other side chains that have been implicated from model building (Fersht et al., 1986). It has been found that catalysis results solely from the use of enzyme–substrate binding energy. In particular, there is a site for binding the γ-phosphate of ATP in the transition state but not the ground state (Leatherbarrow et al., 1985). This site involves the first histidine of the HIGH region and encompasses Thr_{40}-Ala_{41}-Asp_{42}-Ser_{43}-Leu_{44}-His_{45}-Ile_{46}-Gly_{47}-His_{48}. Residue Thr-40 is another key residue in the γ-phosphate binding site: the hydroxyl group makes a hydrogen bond with an oxygen of the phosphate, as does His-45. A similar extended sequence has been located in a number of aminoacyl-tRNA synthetases (Figure 1). But, there are two important differences. First, the crucial threonine residue in the valyl-tRNA synthetase is one position closer to the histidine (Thr-52 and His-56). Second, the threonine is absent from some other enzymes but is replaced by an asparagine, which is in an equivalent position to the threonine in the valyl-tRNA synthetase. Is this imperfect homology significant? Does it provide transition-state stabilization as seen in the tyrosyl-tRNA synthetase? It is now possible to answer these questions without solution of the three-dimensional structure of each synthetase by protein engineering. In this paper we describe how site-directed mutagenesis was used to probe and evaluate homology and transition-state stabilization in the valyl-tRNA synthetase from *B. stearothermophilus*, which we have recently cloned, sequenced, and expressed (Borgford et al., 1987).

Experimental Procedures

The cloning, sequencing, and expression of the valyl-tRNA synthetase gene (*valS*) from *B. stearothermophilus* has been described elsewhere (Brand & Fersht, 1986; Borgford et al., 1987).

Mutagenesis. A 3.3-kb[1] *Pst*I fragment of the plasmid pTB8, which carries the entire structural portion of the *valS* gene, was cloned into M13mp8, thereby permitting the synthesis of a single-stranded template DNA complementary to the *valS* gene. Oligonucleotide site-directed mutagenesis was performed by the method of Zoller and Smith (1982). Oligonucleotides were synthesized on an Applied Biosystems Model 380B DNA synthesizer. The mutation Thr-52 → Ala-52 was directed by

† This work was funded by the MRC of the U.K.
‡ Present address: Department of Biochemistry, University of Alberta, Edmonton, Canada.
§ Present address: Institut de Chimie Biologique, 67085 Strasbourg Cedex, France.

[1] Abbreviations: kb, kilobase(s); $NaDodSO_4$, sodium dodecyl sulfate; Tris, tris(hydroxymethyl)aminomethane; BisTris, [bis(2-hydroxyethyl)-amino]tris(hydroxymethyl)methane.

0006-2960/87/0426-7246$01.50/0

B. stearo.	VTS	P	N	V	T	G		K	L	H	L	G	H	A	60
E. coli	VTS	P	N	V	T	G		S	L	H	M	G	H	A	53
B. stearo.	YTS	F	D	P	T	A	D	S	L	H	I	G	H	L	49
B. caldo.	YTS	F	D	P	T	A	D	S	L	H	I	G	N	L	49
E. coli	YTS	F	D	P	T	A	D	S	L	H	I	G	H	L	51
E. coli	MTS	P	Y	A	N	G		S	I	H	L	G	H	M	25
E. coli	ITS	P	Y	A	N	G		S	I	H	I	G	H	S	69
E. coli	QTS	P	E	P	N	G		Y	L	H	I	G	H	A	44

FIGURE 1: Sequences upstream to the HIGH [=His-Ile(Leu,-Met)-Gly-His(Asn)] region of various aminoacyl-tRNA synthetases (VTS = valyl-, YTS = tyrosyl-, MTS = methionyl-, ITS = isoleucyl-, and QTS = glutaminyl-tRNA synthetase. *B. stearo.* = *B. stearothermophilus*; *B. caldo.* = *B. caldotenax*).

the oligonucleotide 5′-CCAACGTCG*CCGGCAAA-3′, and the mutation His-56 → Asn-56 was directed by the oligonucleotide 5′-CAAATTGA*ACTTAGGG-3′, where mismatches are indicated by asterisks. Once mutations were identified, double-stranded covalently closed circular replicative-form DNA was isolated from M13 vectors, and entire *Pst*I fragments were reintroduced into the pTB8 vector to permit high-level expression of mutant proteins. The DNA sequence of each mutation was determined by the dideoxy method (Sanger et al., 1980) with a bank of sequencing primers described by Borgford et al. (1987) to verify the mutation and that no adventitious mutations had occurred. Each mutant was purified to homogeneity according to $NaDodSO_4$–polyacrylamide gel electrophoresis.

Kinetic Procedures. All measurements were performed in a standard buffer at 25.0 °C containing 144 mM Tris-HCl (pH 7.78), 10 mM $MgCl_2$, 0.1 mM phenylmethanesulfonyl fluoride, and 14 mM 2-mercaptoethanol. The kinetic constants for activation by mutant enzymes were determined by direct measurement of the pre-steady-state formation of enzyme-bound [^{14}C]valyl adenylate by nitrocellulose filter assays and manual sampling [as for slow mutants of the tyrosyl-tRNA synthetase, essentially as described by Leatherbarrow et al. (1985)]. A solution (125 μL) of the standard buffer containing ATP, [^{14}C]Val, and inorganic pyrophosphatase (0.001 unit/mL) was incubated at 25 °C and prewarmed enzyme (25 μL of 20 μM) added to initiate the reaction. Six aliquots of 20 μL were periodically taken over three half-lives of the reaction, filtered through nitrocellulose filters, washed with 3 mL of buffer, and dried under a lamp, and the retained E·[^{14}C]Val-AMP was assayed by scintillation counting. The end point was measured after 10 half-lives. (E·Val-AMP is quantitatively retained by the filters whereas valine is washed through.) The values of K_M for valine were determined at 20 mM ATP (=saturating) with a range of [^{14}C]Val from 5 to 100 μM. The values of K_M for ATP were similarly determined at 100 μM [^{14}C]Val. The observed rate constant for formation of E·Val-AMP (k_{obsd}) was corrected where necessary for the loss of Val-AMP by dissociation or hydrolysis. [$k_{obsd} = k + k_{dec}$, where k is the rate constant for formation and k_{dec} is the rate constant for loss of Val-AMP. The steady-state level of E·Val-AMP formed is given by $[E_0]k/(k + k_{dec})$.] Pre-steady-state kinetics of pyrophosphorolysis of enzyme-bound valyl adenylate was measured for mutant enzymes by a modification of the procedure of Wells and Fersht (1986), with manual sampling instead of stopped-flow fluorescence. Enzyme-bound [^{14}C]valyl adenylate was prepared by incubating enzyme (0.5 mL, 10 μM) with [^{14}C]valine (60 μM) and Mg-ATP (17 mM) at pH 6.0 in BisTris (130 mM) for 40 min at 25 °C, followed by desalting into the standard pH 7.8 buffer by gel chromatography on Sephadex G-50 (medium, 1 × 15 cm). The first-order rate constants for pyrophosphorolysis of the E·[^{14}C]Val-AMP complexes were determined by the reverse of the assay for formation of E·Val-AMP. Pyrophosphate (up to 10 mM) was added to a solution of 150 μL of the E·[^{14}C]Val-AMP complex, periodically taking 6 × 20-μL samples over three half-lives and determining the residual complex by filtration through nitrocellulose filters, as above. The end point was measured after 10 half-lives. The steady-state constants of wild-type enzyme were determined from pyrophosphate exchange kinetics (Wilkinson et al., 1983). Pyrophosphorolysis of wild-type enzyme-bound valyl adenylate was monitored by stopped flow fluorescence (Fersht et al., 1975). Dissociation constants of valine from E·Val were determined by equilibrium dialysis (Mulvey & Fersht, 1977). The first-order rate constants for dissociation of Val-AMP from E·Val-AMP complexes and for hydrolysis of enzyme-bound Val-AMP were determined by the procedure of Wells et al. (1986).

RESULTS

Mutation of Thr-52 and His-56 results in dramatically lowered rate constants for the formation of enzyme-bound valyl adenylate. The stability of the adenylates, however, is hardly altered: wild-type and mutant enzyme-bound adenylates have half-lifes for decomposition of over 1 h under our standard conditions. Enzyme-bound valyl adenylate accumulates on the mutant enzymes despite the low activity. The accumulation is sufficiently slow that its pre-steady-state kinetics may be monitored by manual sampling as described previously for the tyrosyl-tRNA synthetase (Leatherbarrow et al., 1985). This observed accumulation of the intermediate and availability of pre-steady-state kinetics mean that we can reliably assay debilitated enzymes whose activity would be difficult to assay in the steady state.

Analysis of Kinetics. Mutant enzymes bind 1 mol of valine/mol of enzyme (Figure 2) and also form 1 mol of valyl adenylate. The treatment of pre-steady-state kinetics for the valyl-tRNA synthetase is essentially as described by Leatherbarrow et al. (1985). The first-order rate constant for the formation of E·Val-AMP, k, follows Michaelis–Menten kinetics with respect to varying [Val] at constant [ATP] and vice versa (Figure 3). The kinetic data were analyzed according to eq 1, where K_v is the dissociation constant of valine

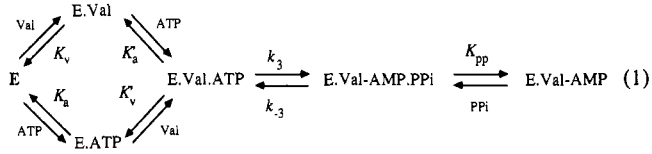

(1)

from the E·Val complex, K'_a is the dissociation constant of ATP from the E·Val·ATP complex, etc. and k_3 and k–3 are the rate constants for the interconversion of ternary complexes. Although the values for mutant enzymes were determined directly by pre-steady-state kinetics, the rate constant for the forward direction for the wild-type valyl-tRNA synthetase (k_3) could not be measured by stopped-flow fluorescence as described for the wild-type tyrosyl-tRNA synthetase. There is a decrease of about 15–20% in tryptophan fluorescence on the binding of valine, but there is no observable change accompanying k_3. However, pyrophosphorolysis of the enzyme-bound valyl adenylate complex in the absence of valine may be monitored by fluorescence because there is rapid dissociation

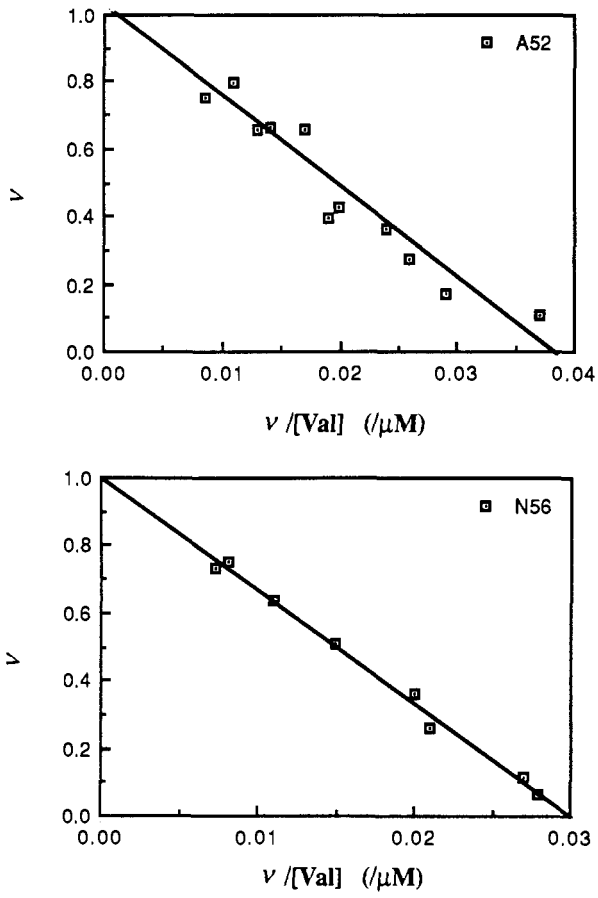

FIGURE 2: Scatchard plots of stoichiometry of binding of valine, ν, against ν/[Val] determined by equilibrium dialysis experiments on the mutants Thr → Ala-52 (upper) and His → Asn-56 (lower).

of valine after the formation of E·Val·ATP. The consequent increase of some 18% in fluorescence in the millisecond time range allows determination of k_{-3} and K_{pp}. The value of k_3 for wild-type enzyme is related to the value of k_{cat} for pyrophosphate exchange measured at a given concentration of pyrophosphate by $k_{cat} = k_3k'_{-3}/(k_3 + k'_{-3})$, where $k'_{-3} = k_{-3}[PP_i]/(K_{pp} + [PP_i])$. Similarly, the value of K_M for pyrophosphate exchange at saturating tyrosine is related to the value of K'_a by $K_M = K'_ak'_{-3}/(k_3 + k'_{-3})$. This allows calculation of k_3 ad K'_a from the combination of pyrophosphate exchange kinetics and pre-steady-state measurements of k_{-3} and K_{pp} (Table I).

Mutation of Thr → Ala-52 reduces k_3 by a factor of 5×10^4 (Table I). The value of K_v is hardly affected, and the value of K'_a is lowered by a factor of 5. Pyrophosphate binding becomes immeasurably weak, and the composite rate constant k_{-3}/K_{pp} decreases by 6×10^4. Mutation of His → Asn-56 reduces k_3 by a factor of 6400, hardly affects K_v, and weakens the binding of ATP by a factor of 2.5. The binding of pyrophosphate becomes immeasurably weak, and the composite rate constant k_{-3}/K_{pp} is lowered by a factor of 3000.

Difference Energy Diagrams. The free energy profiles for all three enzymes [i.e., the energy levels of the enzyme-bound complexes E·Val, E·Val·ATP, E[Val-ATP] (=transition state), E·Val-AMP·PP_i, and E·Val-AMP] were calculated according to Wells and Fersht (1986). The energy level of each complex of wild-type enzyme was subtracted from the energy level of the respective complex of mutant to construct the difference energy profile (Figure 4). The difference energy diagram directly indicates how mutation affects the energy level of each intermediate. Also included in Figure 4 are the difference energies of the analogous mutants in the tyrosyl-tRNA synthetase (R. J. Leatherbarrow and A. R. Fersht, unpublished results) for comparison. It is seen in Figure 4 that mutation has only small effects on the binding of Val, ATP, and Val-AMP. The energy of the transition state (E[Val-ATP]) is greatly raised on mutation. The binding of magnesium pyrophosphate to the mutant Val-AMP complexes is so weakened

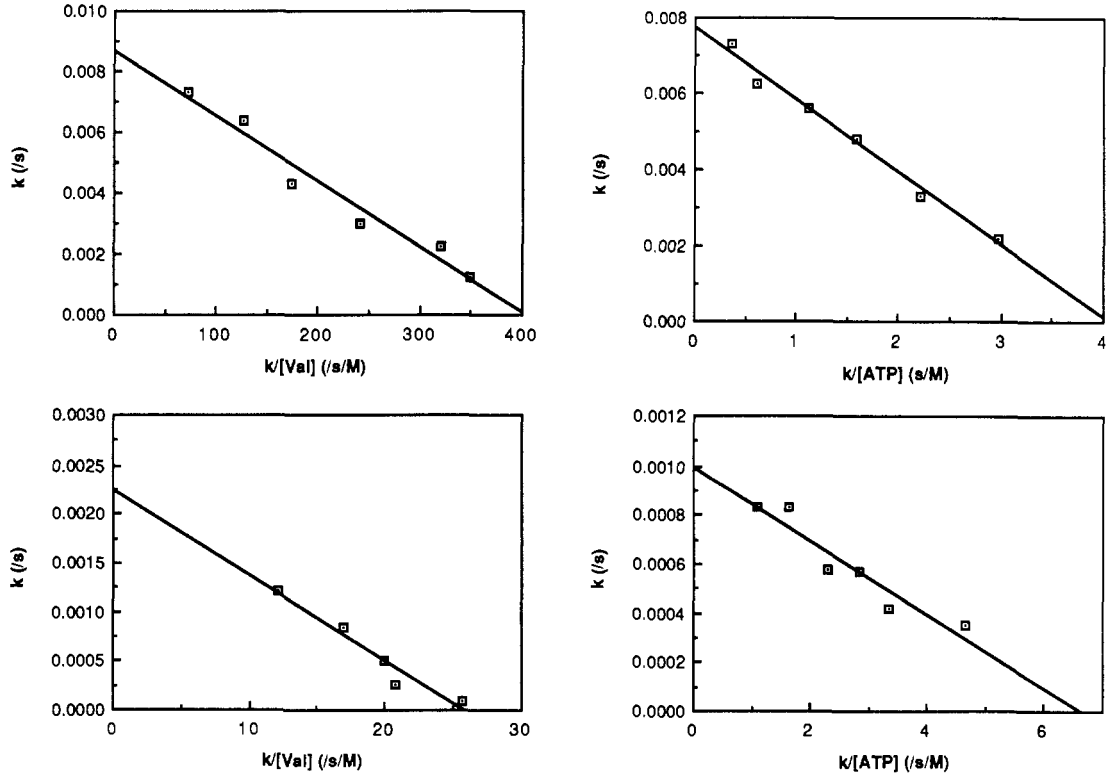

FIGURE 3: Determination of values of k_3, K'_a, and K'_v from Eadie–Hofstee plots of the first-order rate constants, k, for the formation of E·[^{14}C]Val-AMP by the mutants His → Asn-56 (upper) and Thr → Ala-52 (lower). The value for K_M for ATP with Thr → Ala-52 was determined at 100 μM valine. This is only just over the K_M for the amino acid, and so the value of k extrapolated to infinite [ATP] is only about $k_3/2$.

Table I: Kinetic Constants of Wild-Type and Mutant Valyl-tRNA Synthetases[a]

enzyme	K_v (μM)	K'_a (μM)	k_3 (s^{-1})	k_{-3} (s^{-1})	K_{pp} (μM)	k_{-3}/K_{pp} (s^{-1} M^{-1})	k_{diss} (s^{-1})[b]	k_{hyd} (s^{-1})[c]
wild type	20	780[d]	54[d]	80	210	3.8×10^5	6.0×10^{-4}	1.2×10^{-4}
Thr → Ala-52	26[e]	173	0.002			6.3	3.7×10^{-4}	1.1×10^{-4}
His → Asn56	33[f]	2000	0.01			121	5.2×10^{-4}	1.3×10^{-4}

[a] Experiments performed in standard buffer at 25 °C and pH 7.78. Rate and dissociation constants defined in eq 1. [b] Rate constant for dissociation of valyl adenylate from the E·Val-AMP complex. [c] Rate constant for hydrolysis of E·Val-AMP. [d] Calculated from pyrophosphate exchange data as described in the text (k_{cat} = 31 s^{-1}, $K_{M(ATP)}$ = 450 μM). [e] The value of K'_v, the dissociation constant of valine from the E·Val·ATP complex is 90 μM. [f] K'_v is 25 μM.

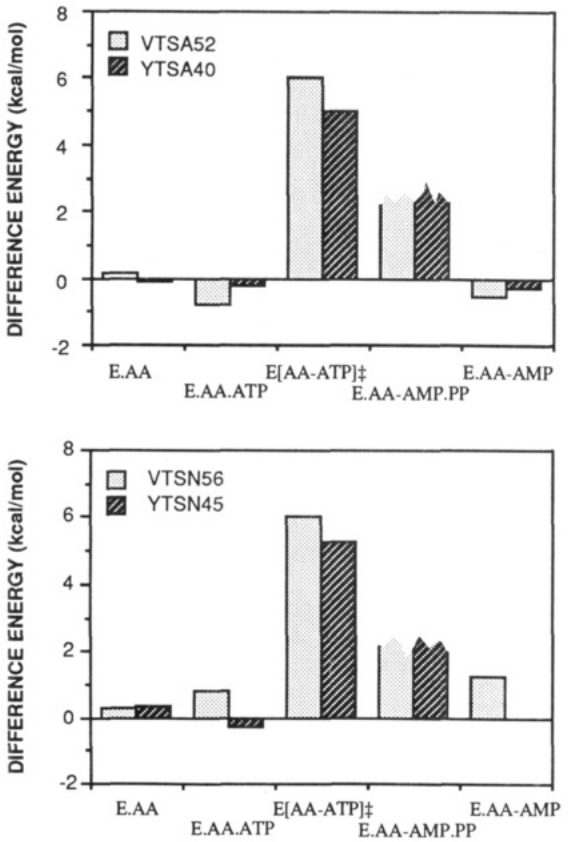

FIGURE 4: Difference free energy profiles (Gibbs free energy levels of complexes of mutant enzymes minus those for wild type). (Upper) Mutation of Thr → Ala-52 in the valyl-tRNA synthetase compared with Thr → Ala-40 in the tyrosyl-tRNA synthetase. (lower) Mutation of His → Asn-56 in the valyl-tRNA synthetase compared with His → Ala-45 in the tyrosyl-tRNA synthetase. Data on the tyrosyl-tRNA synthetase are unpublished results of R. J. Leatherbarrow and A. R. Fersht. AA = Val or Tyr; E[AA-ATP]‡ = transition state for chemical step. The jagged top to the difference energies of the E·AA-AMP·PP_i complex represents a minimum value since the dissociation constants of PP_i are immeasurably high.

that the dissociation constant becomes immeasurable high. The energy level of each mutant E·Val-AMP·PP_i complex is raised by at least 2 kcal/mol.

Discussion

It is immediately obvious on examination of the difference energy diagrams (Figure 4) that mutation of either Thr-52 or His-56 of the valyl-tRNA synthetase has remarkably similar consequences to the mutation of Thr-40 and His-45 of the tyrosyl synthetase. The energy levels of the E·Val, E·Val·ATP, and E·Val-AMP complexes are hardly affected, but the transition-state (E[Val-ATP]‡) and E·Val-AMP·PP_i complexes have greatly raised energy levels. As the interactions in E·Val-AMP are relatively unaffected, the effects in the E·Val-AMP·PP_i complexes must be due to interactions with PP_i. Thr-52 and His-56 must, therefore, be forming a binding site for the pyrophosphate moiety of ATP in the transition state and for pyrophosphate in pyrophosphorolysis. By analogy with the tyrosyl-tRNA synthetase, this must be the binding site for the γ-phosphate of ATP. The small, imperfect homology around the HIGH region of the aminoacyl-tRNA synthetase (Figure 1) is, therefore, significant, and residues Thr-52 and His-56 do contribute to transition-state stabilization.

Residues Thr-40 and His-45 in the tyrosyl-tRNA synthetase are in a loop extending from residue 35 to residue 46, which connects an α-helix to a strand of β-sheet. Loops are among the most flexible elements of protein structure. If Thr-52 and His-56 are in an equivalent loop, then perhaps the flexibility accommodates the difference in separation between the two amino acids compared with the tyrosyl-tRNA synthetase. It is tempting to hypothesize that a connecting loop exists in the valyl-tRNA synthetase, especially as the first two residues of the α-helix in tyrosyl-tRNA synthetase, the G and H of the HIGH region, are present in the valyl-tRNA synthetase, as in the other homologies (Figure 1).

This study shows the power of site-directed mutagenesis for testing proposed homologies. Further, given the wealth of information now available from mutagenesis of the tyrosyl-tRNA synthetase, it should be possible to map out by suitable mutagenesis experiments some regions of the valyl-tRNA synthetase that are functionally equivalent. In this way, the three-dimensional structure of regions of the enzyme may be reconstructed in conjunction with suitable modeling procedures.

Acknowledgments

We thank Tim Wells for performing the stopped-flow measurements of the pyrophosphorolysis of wild-type E·Val-AMP complex.

Registry No. Thr, 72-19-5; Ala, 56-41-7; His, 71-00-1; Asn, 70-47-3; Val, 72-18-4; ATP, 56-65-5; Val-AMP, 52435-65-1; CCA-ACGTCGCCGGCAAA, 110773-01-8; CAAATTGAACTTAGGG, 110743-47-0; aminoacyl-tRNA synthetase, 9028-02-8; valyl-tRNA synthetase, 9023-47-6.

References

Borgford, T. J., Brand, N. J., Gray, T. E., & Fersht, A. R. (1987) *Biochemistry 26*, 2480–2460.

Brand, N. J., & Fersht, A. R. (1986) *Gene 44*, 139–142.

Brick, P., & Blow, D. M. (1987) *J. Mol. Biol. 194*, 287–297.

Fersht, A. R., Mulvey, R. S., & Koch, G. L. E. (1975) *Biochemistry 14*, 13–18.

Fersht, A. R., Leatherbarrow, R. J., & Wells, T. N. C. (1986) *Trends Biochem. Sci. (Pers. Ed.) 11*, 321–325.

Leatherbarrow, R. J., Fersht, A. R., & Winter, G. (1985) *Proc. Natl. Acad. Sci. U.S.A. 82*, 7840–7844.

Mulvey, R. S., & Fersht, A. R. (1977) *Biochemistry 16*, 4005–4013.

Sanger, F., Coulson, A. R., Barrell, B. G., Smith, A. J. H., & Roe, B. A. (1980) *J. Mol. Biol. 143*, 161–178.

Schimmel, P. R., & Soll, D. (1979) *Annu. Rev. Biochem. 48*, 601–648.

Wells, T. N. C., & Fersht, A. R. (1986) *Biochemistry 25*, 1181–1186.
Wells, T. N. C., Ho, C. K., & Fersht, A. R. (1986) *Biochemistry 25*, 6603–6608.
Wilkinson, A. J., Fersht, A. R., Blow, D. M., & Winter, G. (1983) *Biochemistry 22*, 3581–3586.
Zoller, M. J., & Smith, M. (1982) *Nucleic Acids Res. 10*, 6487–6500.

Thermodynamic Analysis of Inducer Binding to the Lactose Repressor Protein: Contributions of Galactosyl Hydroxyl Groups and β Substituents†

Artemis E. Chakerian, John S. Olson, and Kathleen Shive Matthews*
Department of Biochemistry, Rice University, Houston, Texas 77251
Received February 18, 1987; Revised Manuscript Received June 30, 1987

ABSTRACT: Kinetic and equilibrium studies of the binding of modified β-D-galactoside sugars to the *lac* repressor were carried out to generate thermodynamic data for protein–inducer interactions. The energetic contributions of the galactosyl hydroxyl groups to binding were assessed by using a series of methyl deoxyfluoro-β-D-galactosides. The C-3 and C-6 hydroxyls contributed ≤ -2.3 and -1.7 ± 0.3 kcal/mol to the binding free energy change, respectively, whereas the C-4 hydroxyl provided only a nominal contribution (-0.1 ± 0.2 kcal/mol). Favorable contributions to the total binding free energy change were observed for replacement of *O*-methyl by *S*-methyl at the β-anomeric position and for *S*-methyl by *S*-isopropyl. Negative $\Delta H°$ values characteristic of protein–sugar complexes [Quiocho, F. A. (1986) *Annu. Rev. Biochem. 55*, 287–315] were observed for a series of β-D-galactosides differing at the β-glycosidic position. A decrease in $\Delta H°$ of ~6 kcal/mol upon replacement of the *O*-methyl substituent by *S*-methyl indicates a substantial increase in van der Waals' interactions and/or hydrogen bonding in this region of the ligand binding site. The more favorable free energy change for the binding of the *S*-isopropyl vs *S*-methyl compound is due mainly to more positive entropic contributions, consistent with an increase in apolar interactions. Thermodynamic parameters for isopropyl β-D-thiogalactoside (IPTG) binding at neutral pH are in agreement with previously published results [Butler, A. P., Revzin, A., & von Hippel, P. H. (1977) *Biochemistry 16*, 4757–4768; Donner, J., Caruthers, M. H., & Gill, S. J. (1982) *J. Biol. Chem. 257*, 14826–14829]. Arrhenius plots of kinetic rate constants for the binding of IPTG, methyl β-D-galactoside, and methyl β-D-thiogalactoside to the repressor revealed a protein structural transition at 12 °C. All of the experimental data are consistent with the hypothetical sugar binding site for repressor protein proposed by Sams et al. (1984) [Sams, C. F., Vyas, N. K., Quiocho, F. A., & Matthews, K. S. (1984) *Nature (London) 310*, 429–430].

Most effectors of the *lac* operon, either inducers or antiinducers, are β-D-galactosides (Monod et al., 1951; Müller-Hill et al., 1964). The in vivo inducer allolactose (1,6-*O*-β-D-galactopyranosyl-D-glucose) has been identified (Jobe & Bourgeois, 1972), and equilibrium association constants for the binding of an extensive series of β-D-galactoside derivatives to the *lac* repressor protein (Table I) have been determined (Barkley et al., 1975). Kinetic and equilibrium parameters for isopropyl β-D-thiogalactoside binding to *lac* repressor have been examined by fluorescence, visible and ultraviolet spectroscopy, and equilibrium dialysis (Friedman et al., 1976, 1977); the similarity in values obtained by these different methods confirms that the spectroscopic changes are proportional to the fractional saturation by ligand. However, the structural features of the carbohydrate ligand which determine its role as inducer or antiinducer remain elusive, and the specific amino acid residues contacting the ligand are unknown. Site-directed affinity labeling of the carbohydrate binding site with a series of analogues of D-glucose and D-galactose bearing reactive *N*-bromoacetyl functions at C-1 and C-2 of the pyranose ring was notably unsuccessful, although the absence of reactive amino acid residues is consistent with the repressor's role as a binding protein as opposed to a catalytic protein (Brown, 1979). In the absence of a definitive X-ray crystallographic description of free or liganded repressor protein, alternate methods must be relied upon to generate information about the nature of the protein–ligand interactions.

The availability of a series of methyldeoxyfluoro-substituted β-D-galactoside derivatives provided the opportunity to determine directly the contribution of the sugar hydroxyl groups to binding with repressor (Figure 1A). A hypothetical ligand binding site for lactose repressor (Sams et al., 1984; Figure 1B) has been derived from the solved X-ray crystallographic structure of ligand-bound L-arabinose binding protein (ABP)[1] (Quiocho & Vyas, 1984) and sequence homology between ABP and lactose repressor protein (Müller-Hill, 1983). The model indicates that the hydroxyl groups on C-2, -3, -4, and possibly -6 act as hydrogen-bond donors and acceptors to

† This work was supported by grants from the National Institutes of Health (GM 22441 to K.S.M. and GM 35649 to J.S.O.) and the Robert A. Welch Foundation (C-576 to K.S.M. and C-612 to J.S.O.).
* Correspondence should be addressed to this author.

[1] Abbreviations: ONPF, *o*-nitrophenyl β-D-fucoside; IPTG, isopropyl β-D-thiogalactoside; ABP, arabinose binding protein; DTT, dithiothreitol; EDTA, ethylenediaminetetraacetic acid; Tris-HCl, tris(hydroxymethyl)aminomethane hydrochloride; Hepes, *N*-(2-hydroxyethyl)-piperazine-*N*′-2-ethanesulfonic acid; Gal, galactoside.

0006-2960/87/0426-7250$01.50/0